Numerical study of a calamitic liquid-crystal model: Phase behavior and structure

Giorgio Cinacchi, Luca De Gaetani, and Alessandro Tani
Dipartimento di Chimica, Università di Pisa, Via Risorgimento 35, I-56126 Pisa, Italy
(Received 28 October 2004; published 21 March 2005)

We have studied an idealized calamitic liquid-crystal model, consisting of a linear rigid array of nine soft repulsive spheres, employing both theory and molecular dynamics simulation. The phase behavior (which includes crystalline, smectic, nematic, and isotropic phases) and structure of a collection of these rodlike particles have been determined by molecular dynamics simulation in an isothermal-isobaric ensemble. The liquid crystalline part of the phase diagram has been compared to that emerging from an Onsager-type density-functional theory. We have found a fair agreement between theory and computer simulation results, with a similar accuracy for the smectic to nematic and nematic to isotropic phase transitions.

DOI: 10.1103/PhysRevE.71.031703 PACS number(s): 61.30.Cz, 64.70.Md, 61.20.Ja

I. INTRODUCTION AND DESCRIPTION OF THE MODEL

Among the numerous models of rodlike liquid-crystal (LC) molecules proposed and studied during the last decades, particular attention has been recently pointed toward those composed of spherical beads linked together to give idealized elongated particles. These models can be further differentiated on the basis of the nature of the spherical units, of their connectivity, and of the degree of flexibility of the overall chain.

For example, a number of hard spheres, either tangent or fused with a bond length smaller than the diameter, can be held rigidly along a linear array. The constraint of rigidity can then be removed step by step, allowing a systematic investigation of the role of flexibility. A lot of work has been done on such models by both theory and simulation [1–14]. Most simulations have been carried out via the Monte Carlo (MC) [15] method, with the interest directed basically to phase behavior and phase transitions involving ordered fluids.

Besides hard spheres, also soft spherical beads have been adopted, either repulsive or possessing an additional attractive tail. In Ref. [16] the phase behavior of a system of $N=600$ rigid rodlike particles, each composed of 11 sites and site-site interactions described by a potential of the r^{-12} form, was sketched by molecular dynamics (MD) simulation [15]. This study was extended in Ref. [17], where Gibbs-Duhem integration method was employed to trace phase coexistence lines. The latter work was further extended in Ref. [18], where also the effect of the attractive interactions was considered. Elongated liquid-crystal models made up of linearly connected four Lennard-Jones sites were investigated in Refs. [19] and [20]; the author of the latter comments on the possibility of using these models to study liquid crystals in polymer matrices. Stiff and semiflexible models of this type were also studied in Ref. [21]. The advantage of using soft-core beads is that MD simulations are not technically demanding as in the case of hard-body particles. In these studies, the interest was again almost exclusively focused on static properties, notwithstanding the possibility offered by the MD technique to address dynamical behavior.

Among the theoretical studies [4,6–11] of particular interest is, in our opinion, that of Ref. [7], where it was shown that Onsager density functional theory (DFT) [22] with Parsons scaling [23] is able to give a reliable description of the isotropic to nematic phase transition, even for semiflexible particles, where it was found superior than the well-established Khokhlov-Semenov theory [24–26]. However, all theoretical studies on this type of models have considered spatially homogeneous fluids.

We intend to study the effect of chain flexibility on global LC phase behavior and structure, and on both single-particle and collective dynamical quantities. As a first step of this long-term project, we have studied a system of rigid particles, each one composed of nine fused soft spherical beads (see Fig. 1). The site-site pair interaction is equal to the repulsive part of the the Lennard-Jones potential in the Weeks-Chandler-Andersen (WCA) [27] separation; that is,

$$U(r_{ij}) = \begin{cases} 4\varepsilon\left[\left(\frac{\sigma}{r_{ij}}\right)^{12} - \left(\frac{\sigma}{r_{ij}}\right)^{6} + \frac{1}{4}\right] & r_{ij} \leqslant 2^{1/6}\sigma, \\ 0 & r_{ij} \geqslant 2^{1/6}\sigma. \end{cases} \tag{1}$$

The site-site bond length has been kept equal to 0.6σ so that the length-to-width ratio κ of each particle is ≈ 6. We have assumed $\varepsilon = 6.0 \times 10^{-22}$ J and $\sigma = 3.9$ Å. Each site has a mass $m = 15 \times 1.67 \times 10^{-24}$ g. We have computed the phase behavior of a system of $N=600$ particles employing the MD technique in the isothermal-isobaric ensemble (NPT) and compared the thermodynamical and single-particle structural results of the smectic, nematic, and isotropic phases to those obtained from a simple Parsons theory.

We recapitulate theory in Sec. II; the description is rather detailed for the benefit of the reader unfamiliar with the topic. MD NPT simulations are then described in Sec. III. The presentation and discussion of the results of these calculations follow in Sec. IV. In Sec. V, we draw our conclusions. Dynamical properties (translational and reorientational dy-

FIG. 1. The site-site liquid-crystal model.

namics, viscosity) of the same system will be the object of a subsequent paper.

II. PARSONS THEORY

In the field of liquid-crystal statistical thermodynamics, a role of prime importance is played by the Onsager theory [22], a density functional theory *ante litteram*. In a DFT approach the usual splitting of the Helmhotz free energy F in an ideal part F_{id}, known exactly, and an excess part F_{ex}, which depends on interparticle interactions, is adopted. For a system of N rigid particles (that is whose mechanical state is described by the set of translational coordinates $\mathbf{r}$ and by a set of Euler angles Ω) in a volume V and at a temperature T, the ideal free energy is written as

$$F_{id} = k_B T \int d\mathbf{r} d\Omega \rho(\mathbf{r},\Omega) \ln\left[\frac{\nu_T}{e}\rho(\mathbf{r},\Omega)\right], \tag{2}$$

where k_B is the Boltzmann constant and ν_T the De Broglie thermal volume. It is seen that the ideal free energy is a functional of the single particle density, $\rho(\mathbf{r},\Omega)$. The basic idea of DFT is to assume that also the excess free energy is a functional of $\rho(\mathbf{r},\Omega)$.

In the homogeneous case, one may suppose to express F_{ex} as a virial sum

$$F_{ex} = N k_B T \sum_{n>0} \frac{\rho_0^n}{n} B_{n+1}[f(\Omega)], \tag{3}$$

where $\rho_0 = N/V$ and $B_{n+1}[f(\Omega)]$ are the virial coefficients. They are functionals of the orientational distribution function $f(\Omega)$, normalized to unity, since a system of rigid and anisotropic particles can be seen as an infinitely polydisperse mixture where every component is identified by its orientation in a fixed frame of reference. Onsager observed that, for rodlike particles, the virial sum should converge as the aspect ratio goes to infinity. Thus, only the second virial coefficient has to be retained for needlelike particles. In this case

$$F_{ex} = N k_B T \frac{\rho_0}{2} \int\int d\Omega d\Omega' f(\Omega) f(\Omega') \upsilon(\Omega,\Omega'), \tag{4}$$

where $\upsilon(\Omega,\Omega')$ is minus the spatial integral of the appropriate Mayer function. Equation (4) provides the exact expression of the excess free energy for a homogeneous system of rodlike particles with an infinite aspect ratio. Unfortunately, the convergence of the virial series is not as rapid for elongated particles of arbitrary length-to-width ratio. This was observed by Straley [28], who estimated that the Onsager theory should furnish results of quantitative relevance for $\kappa > 100$, but it is invalid for particles of moderate aspect ratio, such as typical thermotropic mesogenic molecules. Although later calculations [29] showed that the prediction of Ref. [28] are too pessimistic, they, nevertheless, confirmed that truncating the virial series after its leading term produces inaccurate results for particles with κ of the order of magnitude of 1–10.

A way to correct the Onsager theory, avoiding the technically demanding calculation of the higher-order virial coefficients (actually done a few times in the past [30–32]), is to resort to the decoupling approximation of Parsons [23]. It consists of a resummation of the virial series where the second coefficient is calculated exactly and the next ones are approximated by mapping them onto those of a reference fluid of "equivalent" hard spheres; that is,

$$B_n[f(\Omega)] \simeq \frac{B_n^{HS}}{B_2^{HS}} B_2[f(\Omega)], \; n > 2. \tag{5}$$

As a consequence, F_{ex} becomes approximated by the following expression:

$$F_{ex} \simeq F_{ex}^{HS} \frac{B_2[f(\Omega)]}{B_2^{HS}}. \tag{6}$$

Equation (6) would be of little use without a knowledge of F_{ex}^{HS}. Fortunately, it is well known that the performance of the Carnahan-Starling expression [33] for the excess free energy of a hard-sphere fluid is very good. Furthermore, it is a common choice to select as "equivalent" the fluid of hard spheres having the same volume of the particle considered. In our case, the particles are soft and their volume is not a well-defined quantity. However, the shape of our particles closely resembles that of hard spherocylinders, whose excluded volume in the parallel configuration ($B_2^{\parallel}$) is eight times the volume of a single spherocylinder. We have assumed that the same relationship holds for our particles. Equation (6) eventually turns out to be

$$F_{ex} \simeq N k_B T \frac{\rho_0}{2} \frac{1 - \frac{3}{4}\rho_0 v_0}{(1-\rho_0 v_0)^2} B_2[f(\Omega)], \tag{7}$$

being $v_0 = B_2^{\parallel}/8$. The success of Parsons theory to give a faithful account of the thermodynamics of isotropic to nematic phase transition is well documented in the literature [34–37]. The same idea has been applied also to two-dimensional fluids [38,39] and mixtures [40–45].

However, in Ref. [46] it was recognized that a generalization of Eq. (7) to a one-dimensional positionally ordered fluid gives for the nematic to smectic phase transition in hard spherocylinders coexistence data as reasonable as those characterizing the nematic to isotropic phase transition. Furthermore, the level of accuracy reached is at least the same as that obtained with more sophisticated DFTs specifically devised to treat layered phases (see, e.g., Ref. [47]). This was later confirmed in Ref. [36] where the bifurcation points of Ref. [46] were compared to computer simulation data and in Refs. [44] and [45] where the binodal points were calculated and compared to accurate MC simulation results [48].

A generalization of Eq. (7) to spatially inhomogeneous fluid is provided by the following expression:

$$F_{ex} \simeq \frac{k_B T}{2} \frac{1 - \frac{3}{4}\rho_0 v_0}{(1-\rho_0 v_0)^2} \times \int\int\int\int d\mathbf{r} d\Omega d\mathbf{r}' d\Omega' \rho(\mathbf{r},\Omega)\rho(\mathbf{r}',\Omega') \times M(\mathbf{r}'-\mathbf{r},\Omega,\Omega'), \tag{8}$$

where $M(\mathbf{r}'-\mathbf{r},\Omega,\Omega')$ is minus the Mayer function. In the case of smectic A phases of layer spacing $\mathbf{d}$ and whose constituents align preferentially along z, Eq. (8) reduces to

$$\mathbf{f}_{ex} = \frac{F_{ex}}{V} \simeq \frac{k_B T}{2} \frac{1 - \frac{3}{4}\rho_0 v_0}{(1-\rho_0 v_0)^2} \frac{1}{\mathbf{d}} \int_0^{\mathbf{d}} dz \int_{-\infty}^{+\infty} dz' \times \int\int d\Omega d\Omega' \rho(z,\Omega)\rho(z'-z,\Omega')A(z'-z,\Omega,\Omega'), \tag{9}$$

where we have introduced the excess free energy density $\mathbf{f}_{ex}$ and $A\ (z'-z,\Omega,\Omega')$ is the area obtained by integrating on x and y minus the Mayer function of two particles whose centers of mass are located at z and z' in the laboratory frame. Assuming that positional and orientational variables are decoupled, we rewrite Eq. (9) as

$$\mathbf{f}_{ex} \simeq \frac{k_B T}{2} \frac{1 - \frac{3}{4}\rho_0 v_0}{(1-\rho_0 v_0)^2} \frac{1}{\mathbf{d}} \times \int_0^{\mathbf{d}} dz \rho(z) \int_{-\infty}^{+\infty} dz' \rho(z') \alpha(z'-z,[f]), \tag{10}$$

where $\rho(z)$ is the single-particle positional distribution function, normalized as

$$\frac{1}{\mathbf{d}} \int_0^{\mathbf{d}} dz \rho(z) = \rho_0, \tag{11}$$

and

$$\alpha(z'-z,[f]) = \int\int d\Omega d\Omega' f(\Omega) f(\Omega') A(z'-z,\Omega,\Omega') \tag{12}$$

plays the role of an effective two-body potential.

The Helmhotz free energy expression is completed by adding to Eq. (10) the ideal contribution, which in the present case takes the following form:

$$\mathbf{f}_{id} = k_B T \frac{1}{\mathbf{d}} \int_0^{\mathbf{d}} dz \rho(z) \left[\ln\left(\frac{\nu_T \rho(z)}{e} \right) + \int d\Omega f(\Omega) \ln 4\pi f(\Omega) \right]; \tag{13}$$

we have introduced the constant $\ln 4\pi$ so that the value of the orientational mixing entropy for our system of uniaxial particles becomes 0 in the isotropic phase.

From the knowledge of the free energy density one can obtain the value of the chemical potential μ as a function of pressure P and temperature,

$$\mu = \frac{\mathbf{f} + P}{\rho_0}. \tag{14}$$

At given pressure and temperature, the thermodynamically stable phase is that corresponding to the absolute minimum of the chemical potential. At this stage, it requires finding, for every point in the (T,P) plane, the minima of Eq. (14) as a functional of the single-particle spatial density $\rho(z)$ and orientational distribution function $f(\Omega)$. In the homogeneous case and for a second virial theory, this leads to an integral equation of the type

$$\ln K f(\Omega) = -\Psi \int d\Omega' f(\Omega') v(\Omega,\Omega'), \tag{15}$$

where K is determined to ensure that the orientational distribution function is normalized to unity, and Ψ is a prefactor that depends on number density and is derived from that entering the definition of excess free energy in the Onsager and Parsons approximations. Several methods have been proposed to numerically solve Eq. (15), from those based on the expansion of $f(\Omega)$ [49,50] or $\ln f(\Omega)$ [51] in Legendre polynomials to the very reliable iterative technique proposed in Ref. [52]. Alternatively, we can directly minimize free energy by the simulated annealing method of Ref. [53] or, as done by Onsager himself and Straley, by using parametrical trial functions. The methods based on an iterative technique [52,53] have the advantage that no particular form of $f(\Omega)$ has to be assumed, but their application to the inhomogeneous case is not straightforward. Methods based on trial functions, though certainly more approximated, are equally reliable if a judicious choice of the parametrization is done. We have therefore decided to adopt the following parametrization of spatial and orientational distribution functions:

$$\rho(z) \propto \rho_0 \exp\left[\lambda \cos\left(2\pi \frac{z}{\mathbf{d}} \right) \right], \tag{16}$$

and

$$f(\Omega) \propto \exp[\Lambda(\eta) P_2(\cos\theta)], \tag{17}$$

$P_2(\cos\theta)$ being the second Legendre polynomial of the cosine of the polar angle and with the proportionality constants ensuring the respective correct normalization. The functional forms assumed for the distributions are the same arising in the Maier-Saupe and McMillan mean-field theories for nematics [54] and smectics [55]. In addition, we observe that they are consistent with the application of the maximum entropy principle [56] to determine the most probable single-particle distribution function of a system of known smectic order parameter $\tau = \langle \cos(2\pi z/\mathbf{d}) \rangle$ and nematic order parameter $\eta = \langle P_2(\cos\theta) \rangle$. Note that the latter relation establishes a one-to-one correspondence between Λ and η. We have determined the chemical potential as a function of temperature and pressure for the isotropic, nematic, and smectic phases. This was done by minimizing, through a nonlinear routine,

Eq. (14) with respect to: (i) ρ_0, for the isotropic phase, keeping fixed and equal to 0 λ and η and leaving **d** undefined; (ii) ρ_0 and η, for the nematic phase, keeping fixed and equal to 0 λ and leaving **d** undefined; and (iii) ρ_0, η, λ, and **d**, all taken free for the smectic phase.

The integrals involved have been evaluated numerically. Phase coexistence points at several values of temperature have been determined by finding the pressure at which chemical potentials are equal. The results are presented in Sec. IV and confronted with those obtained in the MD simulations, whose technical details are described below.

III. ISOTHERMAL-ISOBARIC MOLECULAR DYNAMICS SIMULATIONS: COMPUTATIONAL DETAILS

We have considered a system of $N=600$ particles. The system has been simulated by the molecular dynamics technique in the isothermal-isobaric ensemble. The Nosé-Hoover thermostat [57] has been used to constrain average temperature to the imposed value. This technique has been coupled with the Parrinello-Rahman method [58], allowing the shape (only in spatially inhomogeneous phases) and the volume of the computational box to fluctuate, thus permitting the system to reach the imposed value of the average pressure. The particle beads are maintained in the configuration described in Sec. I by means of the method of constraints reviewed in Ref. [59]. We have considered two pressures, 1.0 and 2.5 Kbar and several temperatures in the range 50–375 K for the lower pressure and 300–700 K for $P=2.5$ Kbar. At the lowest temperatures, we have started the simulation from a perfect crystal in a hexagonal closed-packed configuration, stretched along the x coordinate of the laboratory frame and with all particles parallel to this direction. The resulting computational box was monoclinic, with the following cell vectors and angles: $\mathbf{a}=(a_x,0,0)$, $\mathbf{b}=(0,b_y,0)$, and $\mathbf{c}=(0,c_y,c_z)$; $\alpha=90°$, $\beta=90°$, and $\gamma=60°$. The initial configuration of the other temperatures has been the final one of the equilibration run of the respective previous temperature. To avoid unphysical rotation of the simulational box, **a** has been constrained to lie on x and **b** to move in the xy plane. The time step employed has been 5 fs. For every state point considered, a thermalization run of 500 ps has been followed by a production run of 1 ns (at selected state points, we have extended the time interval simulated up to 2 ns to check the stability of our results, which has proved very satisfactory) during which averages of thermodynamical and structural properties of interest have been acquired. They include the number density, order parameters, single-particle distribution functions, and a family of pair-correlation functions. The results are presented and discussed below.

IV. RESULTS AND DISCUSSION

We begin the presentation of our results by reporting in Table I the values of the thermodynamical quantities entering the equation of state, i.e., pressure, temperature, and density. The last column contains the symbol of the corresponding type of phase.

Thus, at $P=1.0$ Kbar a crystalline (C) phase is observed up to $T=165$ K, while at $P=2.5$ Kbar it is present up to $T=375$ K. The C phase then undergoes a transition to a smectic (S) phase, between $T=165$ K and $T=175$ K at the lower pressure and between $T=375$ K and $T=400$ K at the higher pressure. The existence of the C-S phase transition is first indicated by the qualitatively different behavior of the layer pair-correlation function $g_l(r)$, together with the qualitatively similar behavior of the parallel pair-correlation function $g_p(r)$. They are shown in Figs. 2(a) and 2(b), respectively, at temperatures of $T=375$ K and $T=400$ K, for a pressure of $P=2.5$ Kbar. The former, in an isothermal-isobaric ensemble, is defined as

$$g_l(r)=\frac{1}{N}\left\langle \frac{1}{\rho}\sum_i\sum_{j>i}\delta(r-|\mathbf{r}_{ij}\times\hat{\mathbf{n}}|)\Theta\left(\mathbf{r}_{ij}\cdot\hat{\mathbf{n}}-\frac{\ell}{2}\right)\right\rangle, \tag{18}$$

where δ and Θ are the Dirac and Heaviside functions, respectively, while $\hat{\mathbf{n}}$ is the director (the direction of preferred orientation), and ℓ is the length of a particle, here assumed to be 22.6 Å. $g_l(r)$ gives information on the positional order within a layer. In a crystalline phase it presents a long-range structure, as that of Fig. 2(a) at $T=375$ K, or, more distinctly, at a lower temperature. The first peak corresponds to in-plane nearest neighbors, while the positions of the two still resolved successive peaks are the mark of an in-plane hexagonal order. $g_l(r)$ at $T=375$ K keeps oscillating at large distances where the function at $T=400$ K already approaches the limiting value of unity. This proves the liquidlike character of the positional order inside a layer of the phase at $T=400$ K. The latter is definitely classified as smectic from the behavior of the parallel pair-correlation function of Fig. 2(b). The *NPT* definition of $g_p(r)$ is

$$g_p(r)=\frac{1}{N}\left\langle \frac{1}{\rho}\sum_i\sum_{j>i}\delta(r-\mathbf{r}_{ij}\cdot\hat{\mathbf{n}})\right\rangle; \tag{19}$$

at both $T=400$ K and $T=375$ K, as well as at lower temperatures, this function, which gives information on positional order along the director, shows an oscillating structure with peaks being lower and wider, as the temperature is increased, and separated by a distance of 22–23 Å.

The conclusions drawn from the analysis of the pair-correlation functions are corroborated by the thermal behavior of the bond orientational order parameter Ψ_6 and of the smectic order parameter τ, shown in Figs. 3(a) and 3(b), respectively, for a pressure of 2.5 Kbar. The former is defined as

$$\Psi_6=\frac{1}{3N}\left|\sum_i\sum_{j\in nn(i)}\exp(i6\vartheta_{ij})\right|, \tag{20}$$

where $j\in nn(i)$ means that j is a nearest neighbor of i and ϑ_{ij} is the angle formed by the projection of $\mathbf{r}_{ij}$ onto a plane normal to the director with an axis in this plane. By construction, we have $\Psi_6=1$ in the case of perfect in plane hexagonal order and $\Psi_6=0$ when that order is completely absent, as in the smectic phase. Intermediate values of Ψ_6 correspond to a reduced in-plane hexagonal order, as it happens in a real hcp

TABLE I. Calculated values for the quantities entering the equation of state of the rigid nine beadlace model.

P (Kbar)	ΔP (Kbar)	T (K)	ΔT (K)	$1000\rho_0$ (Å^{-3})	$1000\Delta\rho_0$ (Å^{-3})	Phase
1.0	0.1	50	5	2.88	0.04	C
1.0	0.1	100	5	2.73	0.03	C
1.0	0.05	150	6	2.53	0.02	C
1.0	0.05	165	5	2.47	0.04	C
1.0	0.03	175	5	2.35	0.02	S
1.0	0.01	200	2	2.09	0.01	N
1.0	0.03	250	4	1.97	0.01	N
1.0	0.05	275	8	1.89	0.02	N/I
1.0	0.07	300	6	1.81	0.04	I
1.0	0.05	325	9	1.78	0.02	I
1.0	0.07	350	9	1.74	0.03	I
1.0	0.07	375	8	1.71	0.03	I
2.5	0.08	300	7	2.79	0.01	C
2.5	0.09	350	9	2.71	0.01	C
2.5	0.09	375	10	2.67	0.015	C
2.5	0.09	400	10	2.50	0.015	S
2.5	0.08	435	12	2.32	0.01	N
2.5	0.08	450	11	2.30	0.01	N
2.5	0.07	500	11	2.23	0.01	N
2.5	0.09	550	14	2.17	0.015	N
2.5	0.08	600	15	2.08	0.015	N/I
2.5	0.09	625	16	2.05	0.015	I
2.5	0.09	650	17	2.02	0.015	I
2.5	0.1	675	18	2.00	0.015	I
2.5	0.1	700	18	1.98	0.015	I

crystal. While at $T=400$ K $\Psi_6=0$, the smectic order parameter τ, most generally defined as

$$\tau = \left| \left\langle \exp\left(i2\pi \frac{z}{\mathbf{d}} \right) \right\rangle \right| \tag{21}$$

is far from being zero. It vanishes at the next temperature examined at $P=2.5$ Kbar, that is $T=435$ K, and at $T=175$ K at the lower pressure investigated. This is a clear symptom that a transition to a positionally homogeneous phase has occurred, as the featureless behavior of the pair-correlation functions further testifies. This liquid phase is to be classified as nematic (N), being nonzero the orientational order parameter η [Fig. 3(c), for $P=2.5$ Kbar]. The latter is a decreasing function of temperature, with a discontinuity at $T\simeq 600$ K, being close to zero beyond. We can assume 600 K as the approximate temperature at which a nematic to isotropic (I) phase transition takes place at $P=2.5$ Kbar. Analogously, the NI phase transition occurs at $T\simeq 275$ K for a pressure of 1 Kbar.

We note that the smectic region is quite narrow, if compared to that exhibited by hard spherocylinders of length-to-width ratio equal to 6 [48]. In the latter case we observe the same sequence of phases; that is, C (2.34) S (1.44) N (1.12) I. We have indicated in parentheses the pressure in reduced unit, $P^*=PD^3/k_BT$ (D is the diameter of the spherocylinder), of the corresponding phase transition. To make a comparison, we can choose for our particles a value of D such that the NI phase transition occurs at the same reduced pressure as in the case of spherocylinders, thus obtaining: C (1.78) S (1.68) N (1.12) I. Smectic phase seems to be destabilized with respect to both the crystalline phase and the nematic phase.

In Fig. 4(a) we plot the liquid-crystal phase diagram in the temperature-pressure plane determined from the theory outlined in Sec. II. When compared to computer experiment results, we see a fair agreement. At a fixed pressure, theory overestimates SN and NI transition temperature by, roughly, 15%. The same level of accuracy is reached for coexistence densities, displayed in Fig. 4(b) as a function of temperature. It is worth noting that the performance of Parsons theory in reproducing thermodynamic quantities of the SN phase transition is essentially the same as in the case of NI phase transition.

Among the approximations contained in theory, the chosen parametrization of the singlet distribution functions can be readily tested. In Fig. 5 $\rho^*(z)=\rho(z)/\rho_0$ calculated in simulation at $P=2.5$ Kbar and $T=300$, 350, 375 K (C phase) and $T=400$ K (S phase) is reported together with the corresponding curve fitted through Eq. (16). A good accord is found at

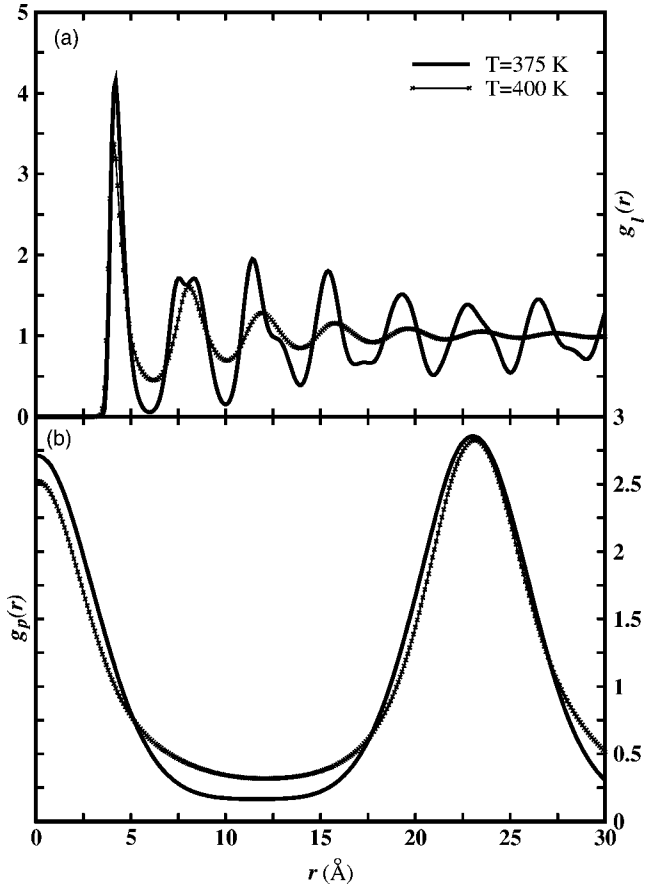

FIG. 2. The layer (a) and parallel (b) pair-correlation functions on either side of the crystal-to-smectic phase transition at $P=2.5$ Kbar.

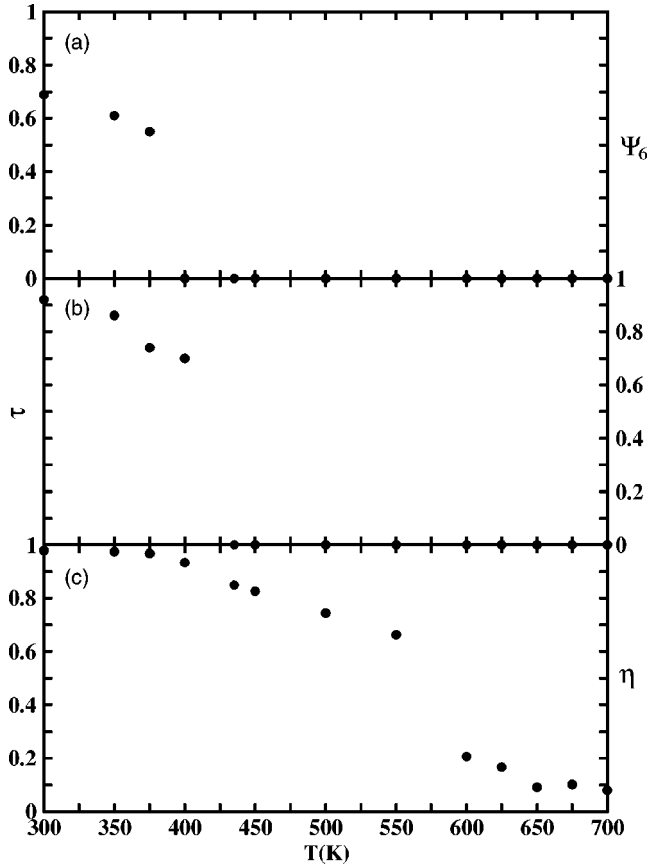

FIG. 3. (a): Bond orientational (Ψ_6); (b) smectic (τ); (c) nematic (η) order parameters, as a function of temperature at $P=2.5$ Kbar.

every temperature. However, the smectic order parameter found in simulations at the SN phase transition (0.70, at $P=2.5$ Kbar) is higher than that calculated by theory (0.57 at $P=2.5$ Kbar); in addition the smectic period **d** found in simulations (22–23 Å) is smaller by a factor of 15% than that obtained in the theoretical procedure. We now pass to the orientational distribution functions. Figure 6 shows $f(\theta)$ at different temperatures, as obtained in simulations at $P=2.5$ Kbar, together with the corresponding curves fitted by Eq. (17). A good agreement is apparent at all temperatures. However, while the orientational order at the SN phase transition is captured rather well by theory ($\eta_S \approx 0.93$, $\eta_N \approx 0.85$ in simulation at $P=2.5$ Kbar versus $\eta_S=0.91$ and $\eta_N=0.87$ from theory at the same pressure), the latter, as expected, overestimates η at the NI phase transition (0.65 versus $\approx 0.2-0.3$). Finally, we note that in the smectic phase the probability to find particles perpendicular to the director (that are supposed to populate intralayer regions) is vanishing small. This may imply that, at least for the present model, the decoupling between positional and orientational variables is a good approximation.

V. SUMMARY AND CONCLUSIVE REMARKS

We have considered a system of elongated particles composed of nine soft repulsive spheres held rigidly on a line. The beads belonging to different particles interact through the repulsive part of the Lennard-Jones potential in the well-known WCA separation. The interaction parameters have been chosen such that ε, the well depth, takes the value of 6.0×10^{-22} J and σ, the range function, that of 3.9 Å. Adjacent beads in any single array are separated by a distance of 2.34 Å, so that the length-to-width ratio of a chain is approximately equal to 6.

The phase behavior of a system of 600 such particles has been studied by molecular dynamics simulations in a isothermal-isobaric ensemble, employing a Nosé-Hoover thermostat coupled with the Parrinello-Rahman technique to vary volume and shape of the computational box. Four phases have been identified: crystalline, smectic, nematic, and isotropic. They have been characterized by discontinuities in density and order parameters and by the shape of the calculated one- and two-particle distribution functions.

The LC thermodynamic phase coexistence data have been confronted with those obtained from a simple Onsager-type density functional theory with a Parsons scaling. The comparison has concerned not only the nematic to isotropic phase transition but also the smectic to nematic one. We have found a fair accord between theory and simulation, with a degree of accuracy similar for both types of phase transition. This could be of interest since Parsons theory was shown to be the best, at present, simple approach providing a reasonable description of the nematic to isotropic phase transition

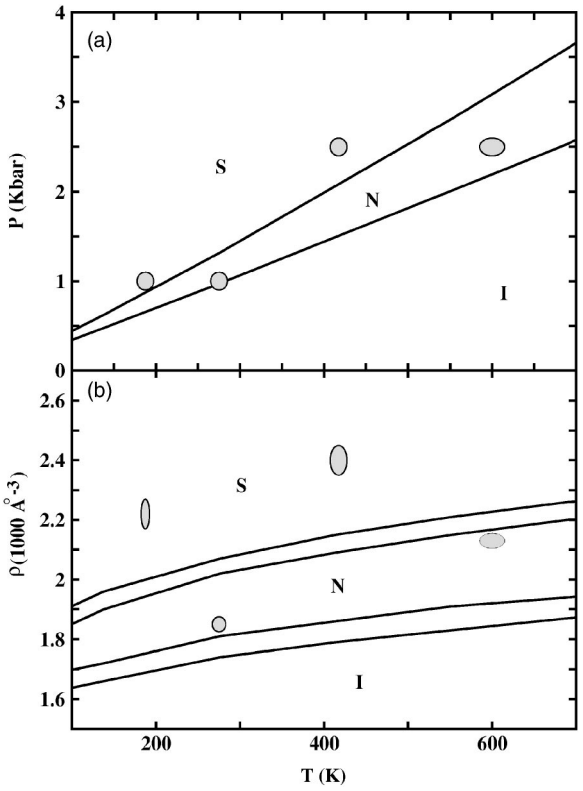

FIG. 4. Theoretical liquid crystal phase diagram. MD simulation data are reported as grey ellipses with width and height determined by the fluctuation of the corresponding quantity.

thermodynamics in short-range repulsive models of liquid crystals. This is well known for rigid bodies but it holds true also for semiflexible particles, as demonstrated in Ref. [7]. Thus, the calculations presented in Ref. [7] can be extended to treat smectic phases formed by semiflexible particles and may be of help in predicting and understanding trends in phase diagrams due to the varying degree of chain flexibility.

There are several ways along which the present theory may be improved. One is a possible better choice of the "volume" of our soft particle, though some arbitrariness is hard to avoid in this case. (Note that if the theory is applied to hard spherocylinders, which have a well-defined volume, the error in reproducing coexistence thermodynamic properties, especially density, is smaller [44,45]). In the search of the optimal "volume" it is difficult not to proceed by "trials and errors." Indeed, we have tried another definition of v_0, namely, that corresponding to take it equal to the effective volume [10] of the hard counterparts of our soft particles (that is, particles composed of nine hard spheres of diameter 3.9 Å held rigid on a line with a bond distance equal to 2.34 Å). We have obtained basically the same results as in Fig. 4, with the density varying less smoothly with temperature in the last case. Another possibility, yet untried, could be to define an effective diameter d^* for the soft beads, interacting through Eq. (1), as

$$d^* = \int_0^\infty 1 - \exp\left(-\frac{U}{k_B T}\right) dr$$

and take v_0 as the volume of a linear array of nine hard spheres with diameter d^* and with a bond distance of $0.6d^*$.

An additional source of error certainly resides in the form of the singlet distribution functions. This form can be improved either by a larger number of parameters or by adopting a different method to minimize free energy (for instance, the Monte Carlo annealing method described in Ref. [53]). However, both of these possible improvements are certainly associated with a considerable increase in the computational cost; (the simulated annealing method may also possess a further disadvantage, i.e., the slowness in reaching stationary points).

Anyway, we believe that the accuracy exhibited by present theory is already acceptable, keeping in mind its aim at reproducing, at least qualitatively, trends in phase diagrams of chain particles. We would like to stress that the resummed second virial theory employed here is intended to give an account of just the thermodynamics of liquid-crystal phase transitions in calamitic model mesogens. We have seen

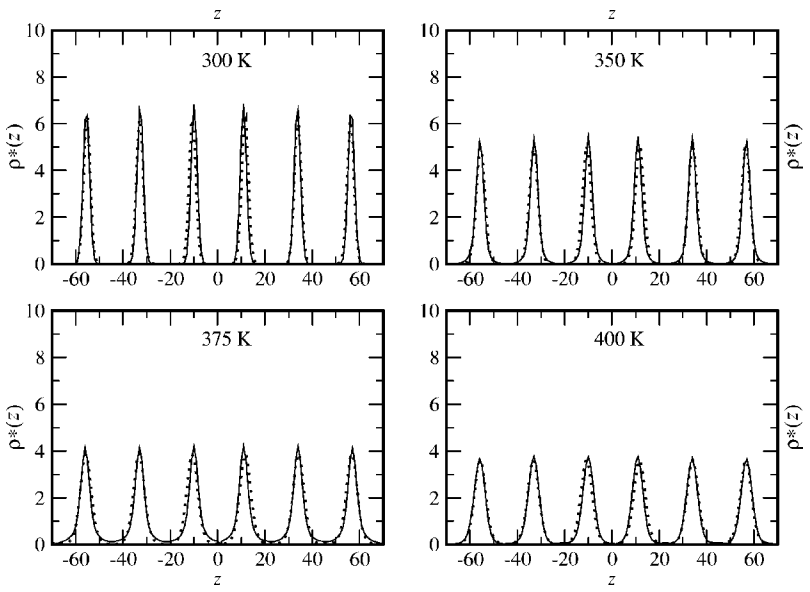

FIG. 5. Positional one-particle distribution functions at $p=2.5$ Kbar and different temperatures, obtained in simulation (solid lines) and fitted via Eq. (16) (dotted lines). The units of the abscissas are Å

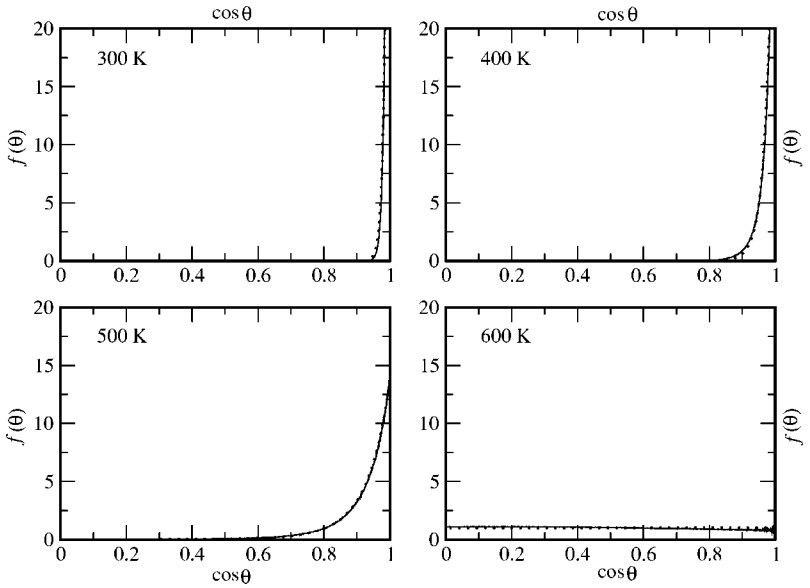

FIG. 6. Orientational distribution function at $P=2.5$ Kbar and several temperatures. Comparison between simulation results (solid lines) and curves fitted via Eq. (17) (dotted lines).

that the agreement with computer experiment results generally gets worse as far as order parameters are concerned. Moreover, we expect that the present theory will be able to reproduce just the gross features of pair-correlation functions. Indeed, the direct correlation function predicted by theory is equal to the Mayer function with a density-dependent prefactor, and this could be true only in the dilute regime [60]. More elaborated density functional theories (such as those based on the weighted density approximation [47,61]) are to be used to address this point. The latter is still rather in its infancy, though some progress has been recently achieved, especially thanks to the evaluation of direct correlation functions of model anisometric particles [62] and its use in the density functional theory formalism [63].

[1] M. Whittle and A. J. Masters, Mol. Phys. **72**, 247 (1991).
[2] M. R. Wilson and M. P. Allen, Mol. Phys. **80**, 277 (1993).
[3] M. R. Wilson, Mol. Phys. **81**, 675 (1994).
[4] C. Vega and S. Lago, J. Chem. Phys. **100**, 6727 (1994).
[5] M. R. Wilson, Mol. Phys. **85**, 193 (1995).
[6] A. Yethiraj and H. Fynewever, Mol. Phys. **93**, 693 (1998).
[7] H. Fynewever and A. Yethiraj, J. Chem. Phys. **108**, 1636 (1998).
[8] D. C. Williamson and G. Jackson, J. Chem. Phys. **108**, 10 294 (1998).
[9] K. M. Jaffer, S. B. Opps, and D. E. Sullivan, J. Chem. Phys. **110**, 11 630 (1999).
[10] S. Varga and I. Szalai, Mol. Phys. **98**, 693 (2000).
[11] K. M. Jaffer, S. B. Opps, D. E. Sullivan, B. G. Nickel, and L. Mederos, J. Chem. Phys. **114**, 3314 (2001).
[12] C. McBride, C. Vega, and L. G. MacDowell, Phys. Rev. E **64**, 011703 (2001).
[13] C. Vega, C. McBride, and L. G. MacDowell, J. Chem. Phys. **115**, 4203 (2001).
[14] C. McBride and C. Vega, J. Chem. Phys. **117**, 10 370 (2002).
[15] M. P. Allen and D. J. Tildesley, *Computer Simulation of Liquids* (Oxford University Press, London, 1987).
[16] G. V. Paolini, G. Ciccotti, and M. Ferrario, Mol. Phys. **80**, 297 (1993).
[17] P. Tian, D. Bedrov, G. D. Smith, and M. Glaser, J. Chem. Phys. **115**, 9055 (2001).
[18] P. Tian, and G. D. Smith, J. Chem. Phys. **116**, 9957 (2002).
[19] M. Yoshida and H. Toriumi, Mol. Cryst. Liq. Cryst. **262**, 525 (1995).
[20] J. C. Lee, J. Chem. Phys. **113**, 6943 (2000).
[21] F. Affouard, M. Kroger, and S. Hess, Phys. Rev. E **54**, 5178 (1996).
[22] L. Onsager, Ann. N.Y. Acad. Sci. **51**, 627 (1949).
[23] J. D. Parsons, Phys. Rev. A **19**, 1225 (1979).
[24] A. R. Khokhlov, Phys. Lett. **68**, 135 (1978).
[25] A. R. Khokhlov and A. N. Semenov, Physica A **108**, 546 (1981).
[26] A. R. Khokhlov and A. N. Semenov, Physica A **112**, 605 (1982).
[27] J. D. Weeks, D. Chandler, and H. C. Andersen, J. Chem. Phys. **54**, 5237 (1971).
[28] J. P. Straley, Mol. Cryst. Liq. Cryst. **24**, 7 (1973).
[29] D. Frenkel, J. Phys. Chem. **91**, 4912 (1987).
[30] B. M. Mulder and D. Frenkel, Mol. Phys. **55**, 1193 (1985).
[31] B. TjiptoMargo and G. T. Evans, J. Chem. Phys. **93**, 4254 (1990).
[32] A. Samborski, G. T. Evans, C. P. Mason, and M. P. Allen, Mol. Phys. **81**, 263 (1994).
[33] N. F. Carnahan and K. E. Starling, J. Chem. Phys. **51**, 635 (1969).
[34] S. D. Lee, J. Chem. Phys. **87**, 4972 (1987).
[35] S. D. Lee, J. Chem. Phys. **89**, 7036 (1988).
[36] S. Mc Grother, D. C. Williamson, and G. Jackson, J. Chem. Phys. **104**, 6755 (1996).
[37] P. J. Camp, C. P. Mason, M. P. Allen, A. A. Khare, and D. A. Kofke, J. Chem. Phys. **105**, 2837 (1996).

[38] S. Varga and I. Szalai, Mol. Phys. **95**, 515 (1998).
[39] S. Varga and I. Szalai, J. Mol. Liq. **85**, 11 (2000).
[40] P. J. Camp and M. P. Allen, Physica A **229**, 410 (1996).
[41] H. H. Wensink, G. J. Vroege, and H. N. W. Lekkerkerker, J. Chem. Phys. **115**, 7319 (2001).
[42] H. H. Wensink, G. J. Vroege, and H. N. W. Lekkerkerker, J. Phys. Chem. B **105**, 10 610 (2001).
[43] A. Galindo, A. J. Haslam, S. Varga, G. Jackson, A. G. Vanakaras, D. J. Photinos, and D. A. Dunmur, J. Chem. Phys. **119**, 5216 (2003).
[44] G. Cinacchi, E. Velasco, and L. Mederos, J. Phys.: Condens. Matter **16**, S2003 (2004).
[45] G. Cinacchi, L. Mederos, and E. Velasco, J. Chem. Phys. **121**, 3854 (2004).
[46] M. Esposito and G. T. Evans, Mol. Phys. **83**, 835 (1994).
[47] E. Velasco, L. Mederos, and D. E. Sullivan, Phys. Rev. E **62**, 3708 (2000).
[48] P. Bolhuis and D. Frenkel, J. Chem. Phys. **106**, 666 (1997).
[49] G. Lasher, J. Chem. Phys. **53**, 4141 (1970).
[50] K. Lakatos, J. Stat. Phys. **2**, 121 (1970).
[51] H. N. W. Lekkerkerker, P. Coulon, R. Van der Haegen, and R. Deblieck, J. Chem. Phys. **80**, 3427 (1984).
[52] J. Herzfeld, A. E. Berger, and J. W. Wingate, Macromolecules **17**, 1718 (1984).
[53] D. C. Williamson and G. Jackson, Mol. Phys. **83**, 603 (1994).
[54] A complete overview of Maier-Saupe theory for nematics and its development is given by G. R. Luckhurst, in *The Molecular Physics of Liquid Crystals*, edited by G. W. Gray and G. R. Luckhurst (Academic, London, 1980), Chap. 4.
[55] See, e.g., P. J. Wojtowicz, in *Introduction to Liquid Crystals*, edited by E. B. Priestly, P. J. Wojtowicz, and P. Sheng (Plenum, New York, 1975), Chap. 7.
[56] E. T. Jaynes, Phys. Rev. **106**, 620 (1957).
[57] S. Nosé, Prog. Theor. Phys. Suppl. **103** 1 (1991).
[58] M. Parrinello and A. Rahman, Phys. Rev. Lett. **45**, 1196 (1980).
[59] G. Ciccotti and J. P. Ryckaert, Comput. Phys. Rep. **4**, 345 (1986).
[60] M. P. Allen, C. P. Mason, E. De Miguel, and J. Stelzer, Phys. Rev. E **52**, R25 (1995).
[61] G. Cinacchi and F. Schmid, J. Phys.: Condens. Matter **14**, 12223 (2002).
[62] N. H. Phuong and F. Schmid, J. Chem. Phys. **119**, 1214 (2003).
[63] D. L. Cheung and F. Schmid, J. Chem. Phys. **120**, 9185 (2004).